

Supporting information

Singlet oxygen is an emissive ligand

Paul Asselin, Adrien Schlachter, and Pierre D. Harvey*

Département de Chimie, Université de Sherbrooke, 2500 Boul. de l'Université, Sherbrooke, QC, J1K 2R1

Contents

Past and present works.....	2
General experimental details.....	2
Procurement and synthesis details.....	2
Safety recommendations	2
Photophysical characterisation in solution.....	3
Singlet oxygen phosphorescence at solid-gas interface.....	4
Atmosphere cycling experiment.....	5
Computations.....	7
General details for computations.....	7
Previous results.....	7
Original computation results (this work).....	8
Geometries.....	8
Orbital contributions and surfaces.....	9
References.....	12

Past and present works

Table S1 Summary of Zn-O distances in various computed and experimental complexes

Entry	Pair or [complex]	Dioxygen multiplicity	Type	Zn-O distance (Å)	Source
1	[¹ ZnTPP ^o + ¹ O ₂ *]	Singlet	Computed	2.36	This work
2	¹ ZnTPP ^o + ³ O ₂ ^o	Triplet	Computed	3.05	This work
3	³ ZnTPP*+ ³ O ₂ ^o	Triplet	Computed	3.08	This work
4	[¹ ZnTPP ^o + ¹ MeOH ^o]	-	Computed	2.30	This work
5	[¹ ZnP ^o + ¹ O ₂ *]	Singlet	Computed	2.411	Rusidy ¹
6	[¹ ZnP ^o + ³ O ₂ ^o]	Triplet	Computed	2.948	Rusidy ¹
7	[³ ZnP*+ ³ O ₂ ^o]	Triplet	Computed	2.825	Rusidy ¹
8	[Distrapped ^a ZnP+O ₂]	Ambiguous ^c	X-ray ^b	2.12	Zhou ²
9	[Distrapped ^a ZnP+O ₂]	Ambiguous ^c	X-ray ^b	2.078	Zhang ³
10	[Distrapped ^a ZnP+MeOH]	-	X-ray ^b	2.167	Zhang ³

^o indicates a ground state and * an excited state.

^a “Distrapped” indicates a pair of -O-alkyl-O- chains, each linking two meso positions.

^b Resolved at low temperatures.

^c While dioxygen prior to the moment of coordination might have been singlet or triplet, the loss of symmetry of the dioxygen molecule likely breaks its π orbital's degeneracy which would favour a globally singlet multiplicity.

General experimental details

Procurement and synthesis details

Porphyrins were purchased from PorphyChem. Solvents and common reagents were purchased from Sigma-Aldrich or Fisher Scientific.

Safety recommendations

Great care should be exercised when handling oxygen and argon cylinders and dispensing gases. All combustibles and potential ignition sources should be moved away from the O₂ cylinder and gas outlet, as higher O₂ concentrations pose an elevated ignition risk and fire hazard. Argon is a simple asphyxiant.

Extra care should be exercised when mixing and handling the air+MeOH_(g) and O_{2(g)}+MeOH_(g) mixtures. They are highly flammable mixtures of fuel and oxidizer, and their ignition can result in an explosion.

Photophysical characterisation in solution

All scans in **Figure S1** were recorded from solutions whose absorbance was adjusted to roughly 0.9 A.U. in 10x10 mm quartz cuvettes. All scans have been normalized to 0-1 save those used to demonstrate quantities. UV-Vis spectra were obtained from a DCM solution with an Agilent 6345 diode-array spectrophotometer. Emission and excitation spectra were obtained from the same solution with an Edinburgh Instruments FLS980 equipped with Xe lamp and single-single monochromators. Scans were corrected for instrument response. 3 scans were averaged for each spectrum.

Singlet oxygen phosphorescence spectra (from DCM and MeOH solutions in sealed 10x10 mm quartz cuvettes) were obtained with a Horiba-PTI QM-400 equipped with Xe lamp, single-single monochromators, and NIR-sensitive R5509-42 PMT housed in a liquid nitrogen-cooled compartment. A 1200 nm longpass filter from Thorlabs was placed between the sample and emission monochromator. Integration time was set to 1-2 seconds and near-maximum slits (50 nm or more where 5-10 are usually sufficient) openings were used. Scans were corrected for instrument response. 10 scans were averaged for emission spectra and 5 scans for excitation spectra.

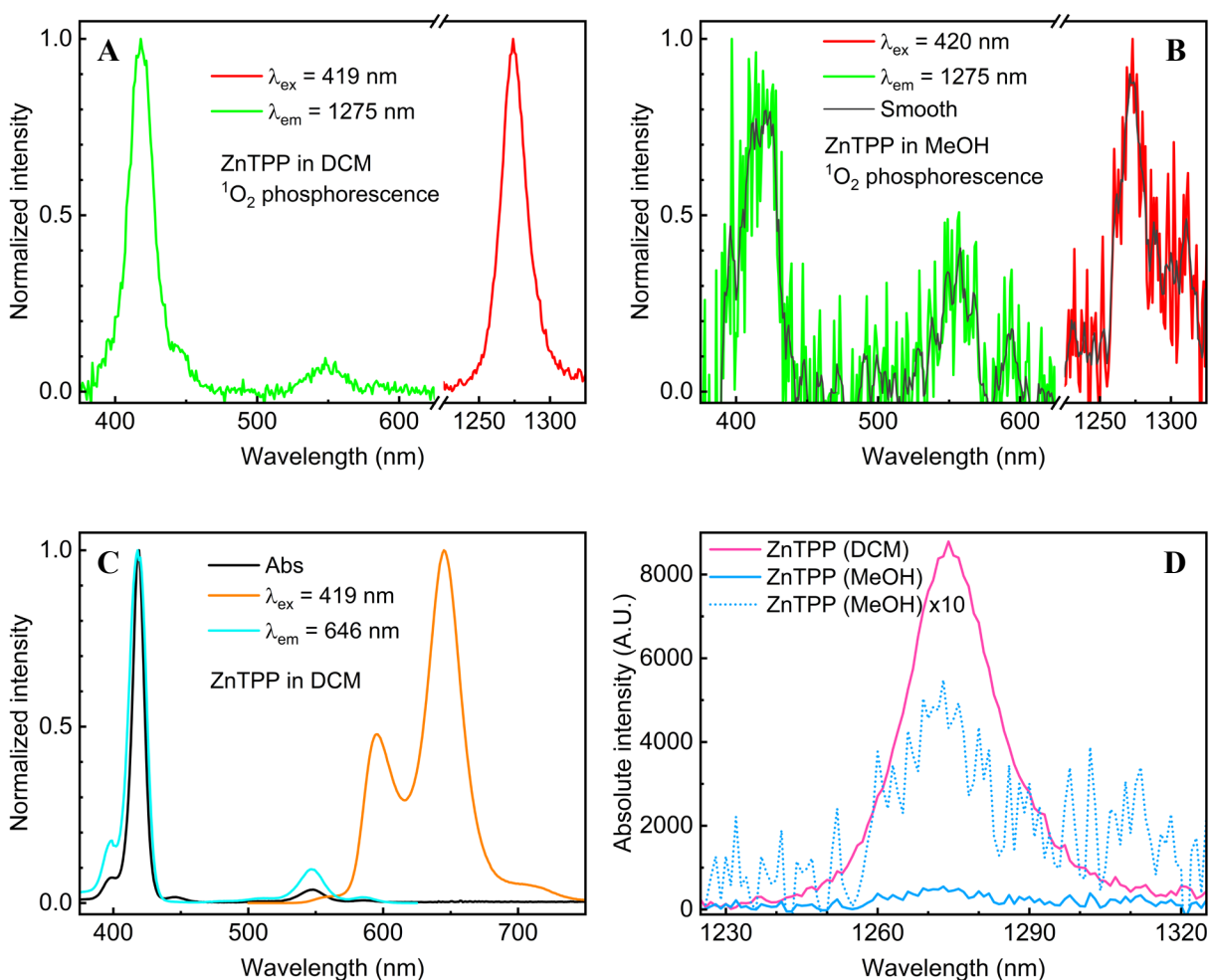


Figure S1: **A and B:** Normalized $^1\text{O}_2$ phosphorescence from dilute ZnTPP in DCM (**A**) and MeOH (**B**). In red, typical $^1\text{O}_2$ phosphorescence spectra, and in green, $^1\text{O}_2$ excitation spectra. **C:**

absorption, emission, and excitation spectra of dilute ZnTPP in DCM. **D**: recorded absolute intensities of $^1\text{O}_2$ phosphorescence in both solvents.

Singlet oxygen phosphorescence at solid-gas interface

Singlet oxygen phosphorescence spectra (from solid/gas interface of neat drop-cast or pressed powders) were obtained with a Horiba-PTI QM-400 equipped with Xe lamp, single-slit monochromators, and NIR-sensitive R5509-42 PMT housed in a liquid nitrogen-cooled compartment. A 335-610 nm bandpass filter from Newport was placed between the excitation monochromator and the sample, while a 1200 nm longpass filter from Thorlabs was placed between the sample and emission monochromator. Integration time was set to 2 seconds and near-maximal (50 nm or more) openings were used. The entire sample compartment could be purged with air, oxygen, or argon.

For time-resolved measurements, the same setup was kept, except for switching the excitation light source to a pulsed Xe lamp, and that the sample compartment was always kept under pure oxygen.

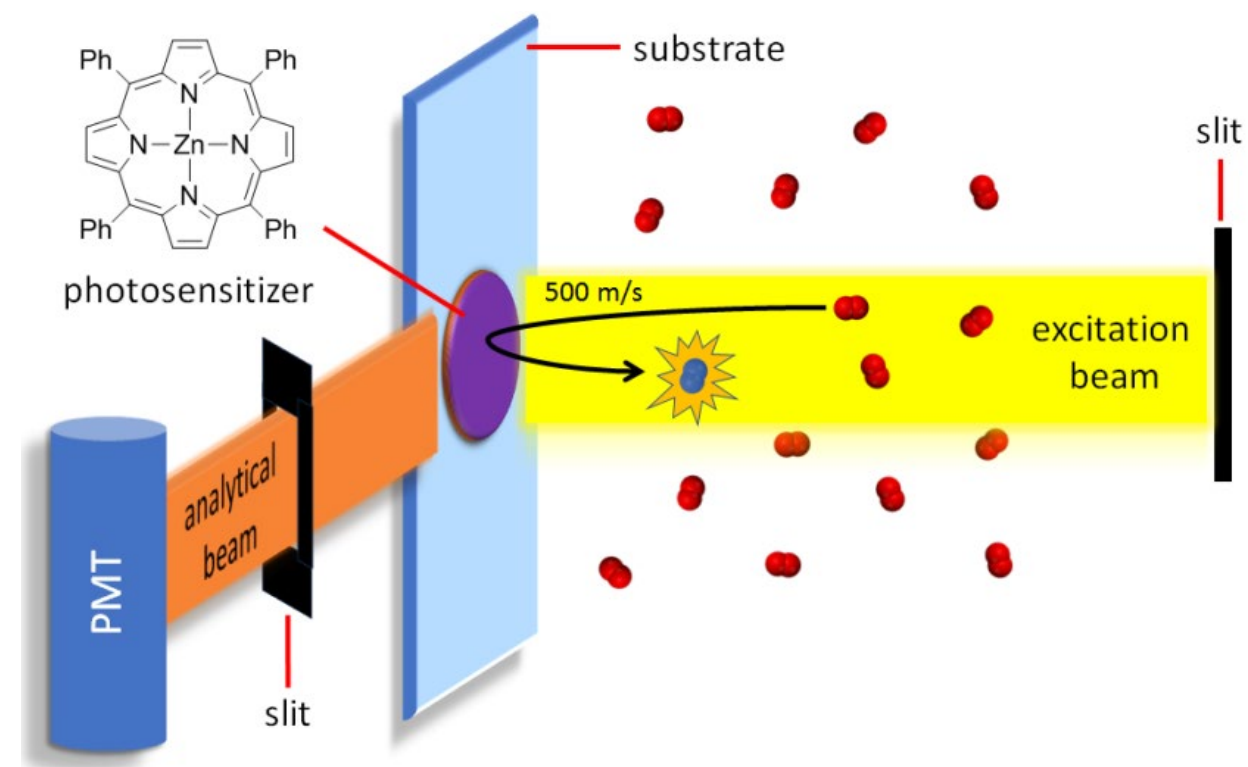


Figure S2 : Experimental setup for solid-gas interface photosensitization and phosphorescence measurements. $^1\text{O}_2$ photosensitization. Diagram: the red and blue molecules are $^3\text{O}_2$ and $^1\text{O}_2$, respectively, and λ_{ex} will generally excite the Soret band. It is noteworthy that the velocity of O_2 at room temperature and an excited state lifetime of 20 μs , for example, predict that the linear distance travelled by $^1\text{O}_2$ after collision is 1 cm. Therefore, even when using very wide slit openings, only $^1\text{O}_2$ near the surface will be detected.

Atmosphere cycling experiment

The coordination experiment summarized in **Figure 1** was conducted on drop-cast (cast a drop, wait for evaporation, cast next drop, repeated several times) ZnTPP from degassed DCM inside a 10x10 mm quartz cuvette, placed in a similar way as the microscope slide in **Figure S2**, as purging a 4 mL volume is much easier, quicker, and safer than purging the entire sample compartment. This results, however in a much trickier sample positioning process as the angle of the cuvette must be adjusted by trial and error until proper signal intensity is observed. To better monitor progress in time, only single scans were recorded for each measurement. Scans were corrected for instrument response.

Following drop casting the cuvette was closed with a septum-cap and purged with a continuous flow (inlet and outlet needles) of pure oxygen for 5 min. The cuvette was then placed in the sample compartment and had its angle adjusted to maximize the signal. Once this was done, the #1 scan was recorded. The cuvette was then purged with a continuous flow of argon for 1 min and scanned again. The remaining signal observed in scan #2 was initially believed to be residual gaseous O₂ in the cuvette (partially correct), so two other purge-scan sequences were performed, with #3 and #4 scans being identical. This was the point where suspicion of a coordinated complex initially arose, as the signal was not only stable, but distinctly above the expected flatline. The cuvette was purged with air for scans #5 and #6, with a stable signal being observed immediately. In the meantime, the test for the coordination hypothesis had been formulated: the cell was purged with 60 mL of methanol-saturated air, prepared by thoroughly shaking several mL of methanol in a large 60 mL syringe filled with air, then draining the excess liquid. The purge-scan sequence was repeated up to scan #10, where a stable flatline was observed. The cuvette was then purged with methanol-saturated oxygen in the same manner and the sequence was repeated up to scan #13, which revealed a small increase in signal, which could not confidently be attributed to singlet oxygen resurgence (increased noise and average baseline value).

Figure 1 was obtained by averaging the data points from 1275 nm to 1285 nm from each scan presented in **Figure S3**. The result of each averaging is the point corresponding to the step #.

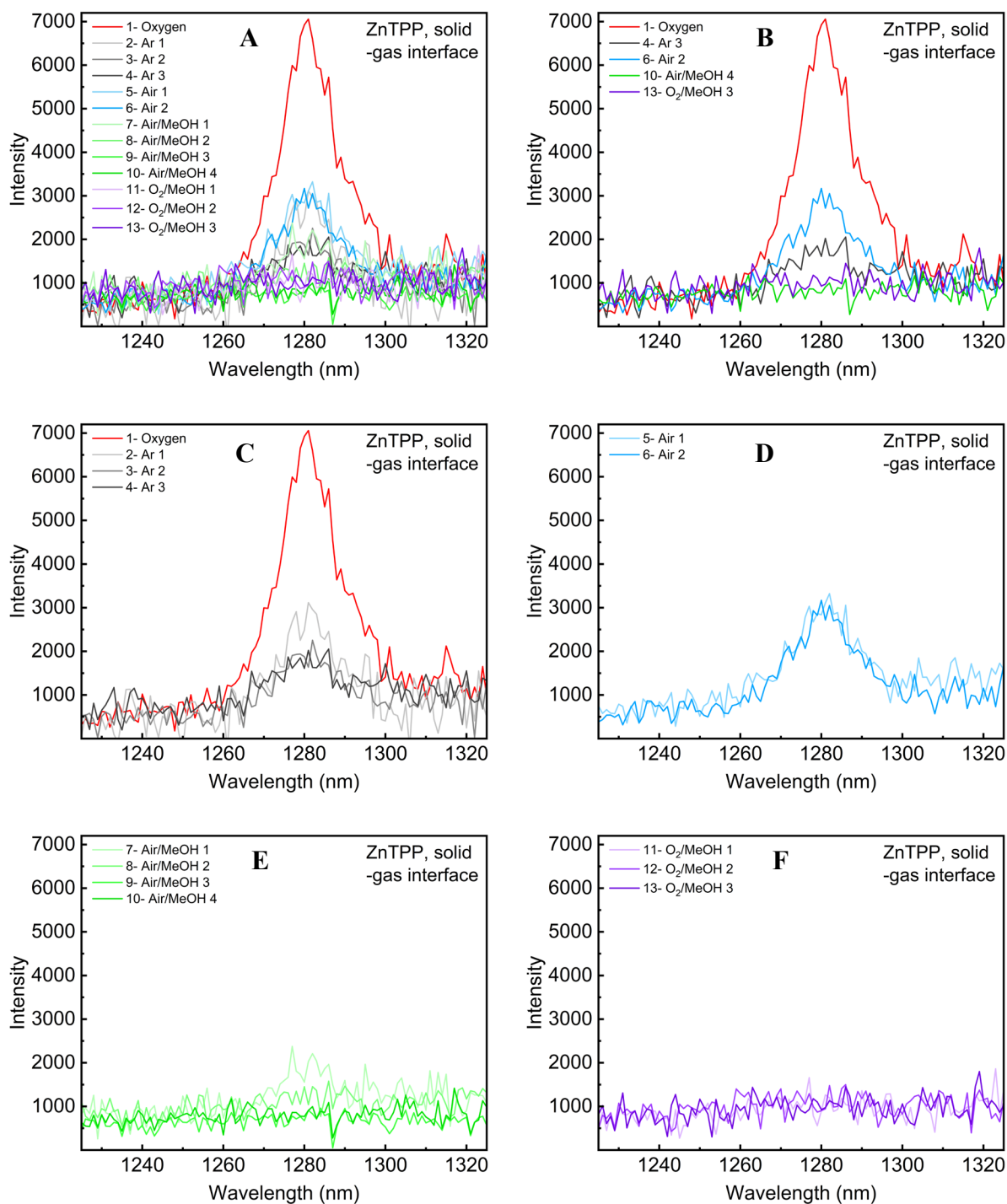


Figure S3 : Raw spectra of the atmosphere cycling experiment. **A**: All scans; **B**: Last scans of each condition once signal has stabilized; **C**: Oxygen and argon scans only; **D**: air scans only; **E**: air/MeOH scans only; **F**: O₂/MeOH scans only.

Computations

General details for computations

All density functional theory (DFT) was performed with Gaussian 16⁴ at *Université de Sherbrooke's Mammouth* supercomputer supported by *Calcul Québec*, part of the Digital Research Alliance of Canada. Geometry optimization calculations were carried out using the B3LYP/genecp method and counterpoise keyword, allowing to differentiate two spin-systems. A 6-31 g (d,p) basis set^{5,6} was used for C, H, N and O atoms, while a LANL2DZ basis set^{7,8} was used for Zn. A photosensitizer (ZnTPP) was optimized starting from a .cif file obtained from structure repositories, to which was added an oxygen molecule to simulate the interactions between the two systems. The system was then optimized using different spin settings to simulate the photosensitization of oxygen, followed by the calculation of electronic absorption spectra. The absence of imaginary frequencies indicates that the counterpoise correction adequate, and the system optimized to a minimal energy configuration. Red corresponds to the positive isosurface, while blue corresponds to the negative one with a contour value of 0.05. Hydrogen atoms linked to carbon atoms were hidden in the figures to increase clarity.

Previous results

The following figure summarizes Rusidy *et. al's*¹ work:

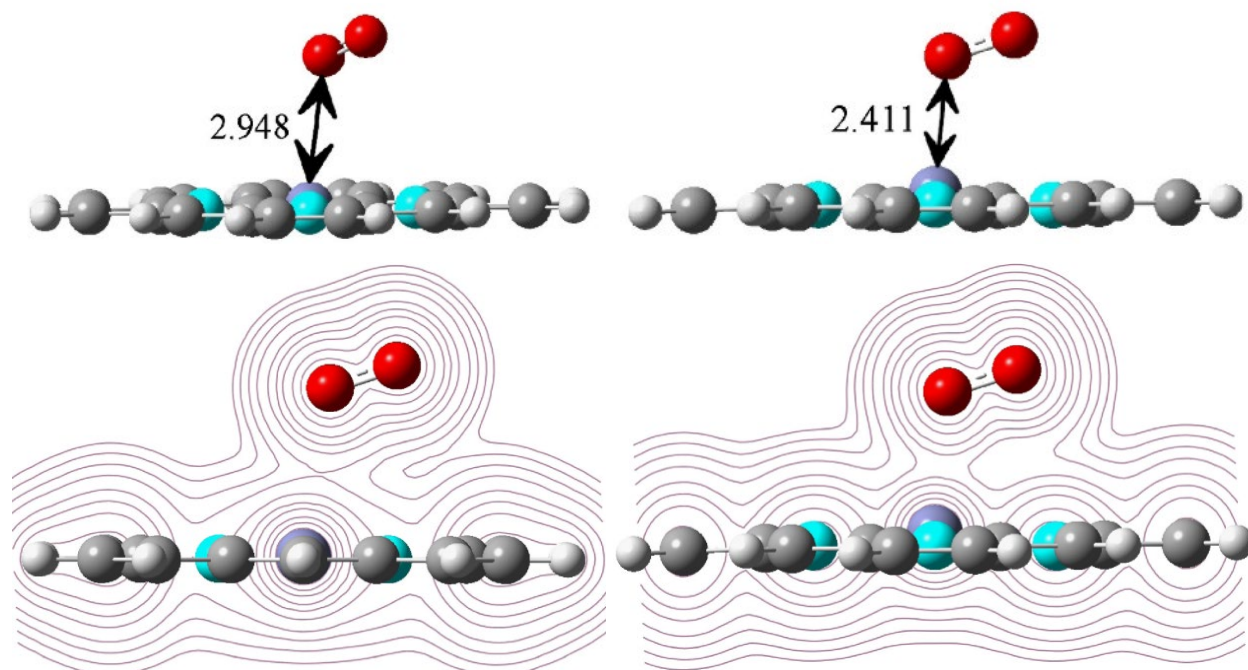


Figure S4: Geometry of the transient $^1\text{ZnP-O}_2$ complex (left $^3\text{O}_2$, right $^1\text{O}_2$) as calculated by Rusidy *et Al.*¹ Distances in Å. Reproduced with permission. Copyright 2012 Physical Society of Japan.

Original computation results (this work)

Geometries

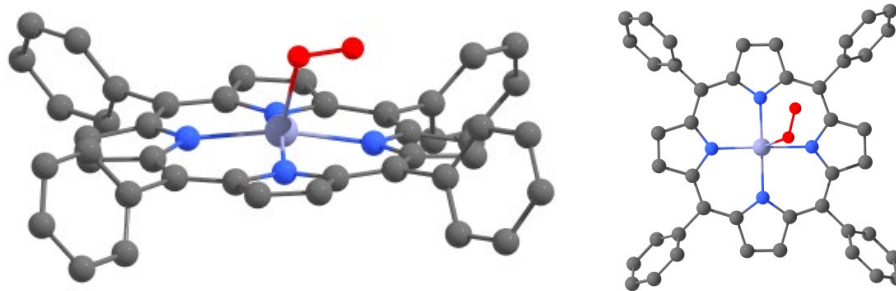


Figure S5: Optimised structure of $[^1\text{ZnTPP}^{\circ}+^1\text{O}_2^*]$ viewed from both side and top. The Zn-O distance is 2.36 Å, the stabilization energy is -45.94 kJ/mol. C-H hydrogens omitted for clarity.

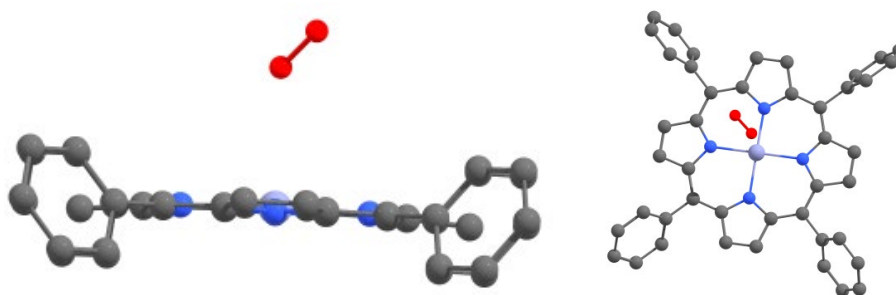


Figure S6: Optimised structure of $^1\text{ZnTPP}^{\circ}+^3\text{O}_2^{\circ}$ viewed from both side top. The Zn-O distance is 3.05 Å, the stabilization energy is 0.63 kJ/mol. C-H hydrogens omitted for clarity.

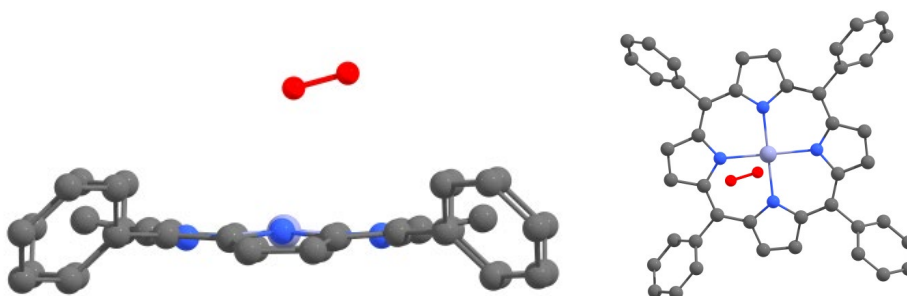


Figure S7: Optimised structure of $^3\text{ZnTPP}^*+^3\text{O}_2^{\circ}$ viewed from the side and top. The Zn-O distance is 3.08 Å, the stabilization energy is 1.96 kJ/mol. C-H hydrogens omitted for clarity.

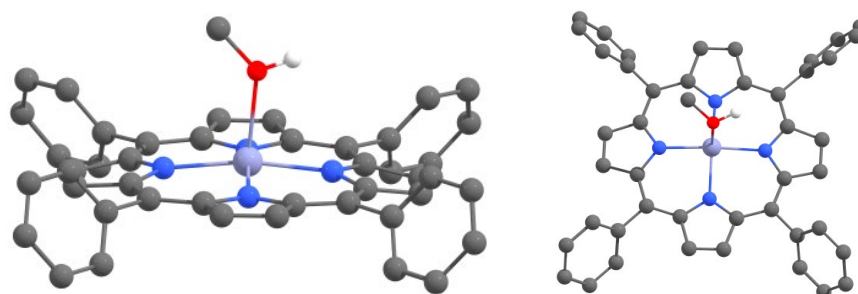


Figure S8 : Optimised structure of $[^1\text{ZnTPP}^{\circ}+^1\text{MeOH}^{\circ}]$ viewed from the side and top. The Zn-O distance is 2.30 Å, the stabilization energy is 37.16 kJ/mol. C-H hydrogens omitted for clarity.

Major contributions of 10% or more are highlighted in blue. Minor contributions of 1-10% are highlighted in yellow.

Table S2: Atomic contributions of the frontier MOs of [¹ZnTPP^o+¹O₂*]

Fragment	H-4	H-3	H-2	H-1	HOMO	LUMO	L+1	L+2	L+3	L+4
Energy (eV)	-6.52	-6.48	-5.52	-5.21	-5.09	-3.49	-2.21	-2.19	-0.74	-0.20
Zn (%)	0.50	0.14	1.85	0.32	0.49	0.53	0.20	0.14	0.01	0.29
Porphyrin (%)	99.03	99.60	14.39	91.25	76.34	24.79	99.13	96.32	99.86	99.66
Oxygen (%)	0.48	0.26	83.76	8.42	23.17	74.68	0.67	3.54	0.13	0.05

Table S3: Atomic contributions of the frontier MOs of ¹ZnTPP*+³O₂.

Fragment	LS-3	LS-2	LS-1	LSOMO	HSOMO	LUMO	L+1	L+2	L+3	L+4
Energy (eV)	-6.41	-5.15	-5.14	-4.91	-4.91	-3.19	-3.11	-2.14	-2.14	-2.14
Zn (%)	0.02	0.00	0.00	1.23	1.09	1.64	0.97	0.14	0.16	0.14
Porphyrin (%)	99.98	100.00	100.00	98.06	98.73	2.06	1.51	99.81	99.84	99.79
Oxygen (%)	0.00	0.00	0.00	0.71	0.18	96.31	97.52	0.05	0.00	0.07

Table S4: Atomic contributions of the frontier MOs of ³ZnTPP*+³O₂.

Fragment	LS-3	LS-2	LS-1	LSOMO	HSOMO	LUMO	L+1	L+2	L+3	L+4
Energy (eV)	-6.05	-5.32	-5.26	-5.13	-3.32	-3.20	-3.11	-2.21	-1.89	-1.82
Zn (%)	0.67	0.78	0.01	0.01	0.17	1.68	0.41	0.10	0.28	0.12
Porphyrin (%)	99.24	99.13	99.99	99.97	99.82	4.60	1.18	99.89	99.71	99.86
Oxygen (%)	0.09	0.09	0.01	0.02	0.01	93.72	98.41	0.01	0.02	0.03

Table S5 : Atomic contributions of the frontier MOs of [¹ZnTPP^o+MeOH^o].

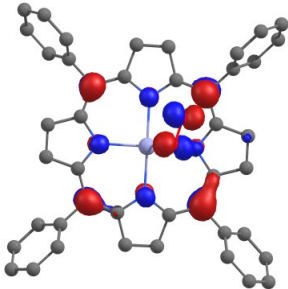
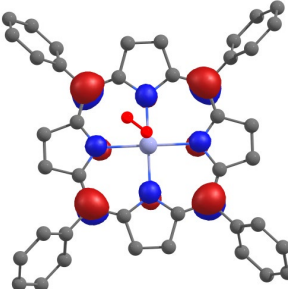
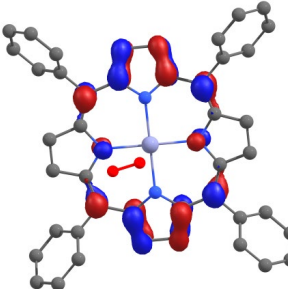
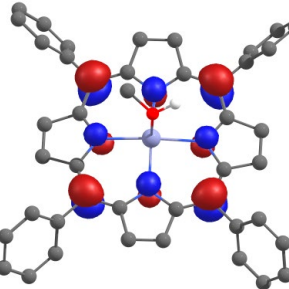
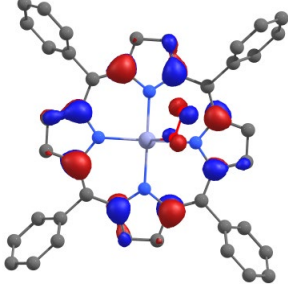
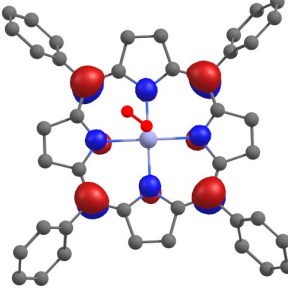
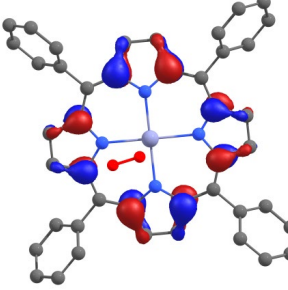
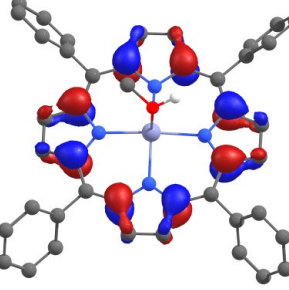
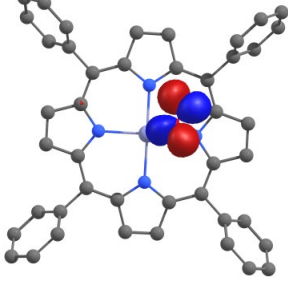
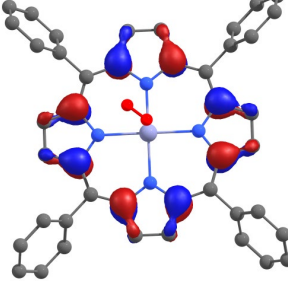
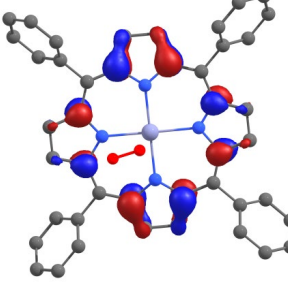
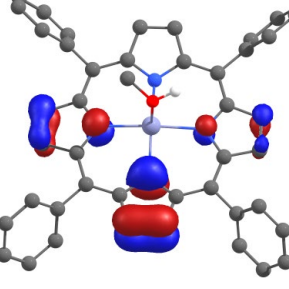
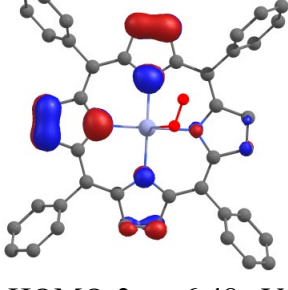
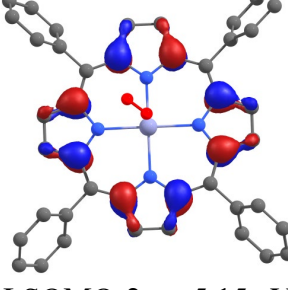
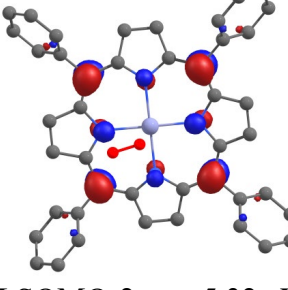
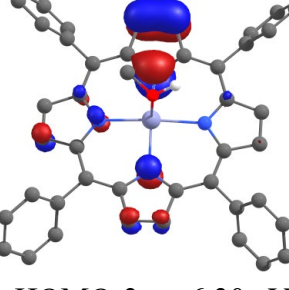
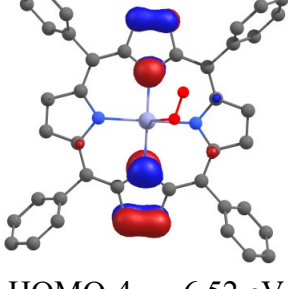
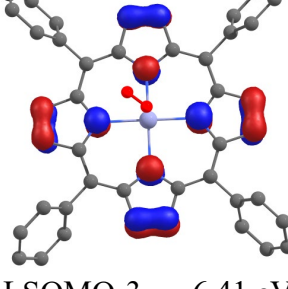
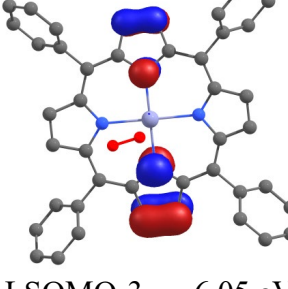
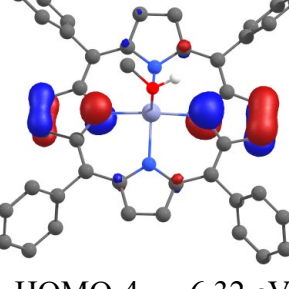
Fragment	H-4	H-3	H-2	H-1	HOMO	LUMO	L+1	L+2	L+3	L+4
Energy (eV)	-6.32	-6.30	-6.26	-5.01	-4.71	-2.02	-2.01	-0.56	-0.05	-0.03
Zn (%)	0.47	0.50	0.15	0.00	0.76	0.23	0.12	0.00	0.50	1.51
Porphyrin (%)	99.23	99.27	99.69	99.96	98.50	99.75	99.81	100.00	99.35	98.43
MeOH (%)	0.30	0.23	0.15	0.03	0.74	0.03	0.07	0.00	0.15	0.06

Next page: orbital surfaces for the four complexes. C-H hydrogens omitted for clarity.

Table S6: Orbital surfaces of [$^1\text{ZnTPP}^\circ + ^1\text{O}_2^*$], $^1\text{ZnTPP}^* + ^3\text{O}_2^\circ$, $^3\text{ZnTPP}^* + ^3\text{O}_2^\circ$, and [$^1\text{ZnTPP}^\circ + ^1\text{MeOH}^\circ$]

$[^1\text{ZnTPP}^\circ + ^1\text{O}_2^*]$	$^1\text{ZnTPP}^* + ^3\text{O}_2^\circ$	$^3\text{ZnTPP}^* + ^3\text{O}_2^\circ$	$[^1\text{ZnTPP}^\circ + ^1\text{MeOH}^\circ]$
 LUMO+4 -0.20 eV	 LUMO+4 -2.14 eV	 LUMO+4 -1.82 eV	 LUMO+4 -0.03 eV
 LUMO+3 -0.74 eV	 LUMO+3 -2.14 eV	 LUMO+3 -1.89 eV	 LUMO+3 -0.05 eV
 LUMO+2 -2.19 eV	 LUMO+2 -2.14 eV	 LUMO+2 -2.21 eV	 LUMO+2 -0.56 eV
 LUMO+1 -2.21 eV	 LUMO+1 -3.11 eV	 LUMO+1 -3.11 eV	 LUMO+1 -2.01 eV
 LUMO -3.49 eV	 LUMO -3.19 eV	 LUMO -3.20 eV	 LUMO -2.02 eV

Continued from previous page

$[^1\text{ZnTPP}^\circ + ^1\text{O}_2]$	$^1\text{ZnTPP}^* + ^3\text{O}_2$	$^3\text{ZnTPP}^* + ^3\text{O}_2$	$^1\text{ZnTPP}^\circ + \text{MeOH}$
 HOMO -5.09 eV	 HSOMO -4.91 eV	 HSOMO -3.32 eV	 HOMO -4.71 eV
 HOMO-1 -5.21 eV	 LSOMO -4.91 eV	 LSOMO -5.13 eV	 HOMO-1 -5.01 eV
 HOMO-2 -5.52 eV	 LSOMO-1 -5.14 eV	 LSOMO-1 -5.26 eV	 HOMO-2 -6.26 eV
 HOMO-3 -6.48 eV	 LSOMO-2 -5.15 eV	 LSOMO-2 -5.32 eV	 HOMO-3 -6.30 eV
 HOMO-4 -6.52 eV	 LSOMO-3 -6.41 eV	 LSOMO-3 -6.05 eV	 HOMO-4 -6.32 eV

References

- (1) Rusydi, F.; Kemal Agusta, M.; Gandaryus Saputro, A.; Kasai, H. A First Principles Study on Zinc–Porphyrin Interaction with O₂ in Zinc–Porphyrin(Oxygen) Complex. *J. Phys. Soc. Japan* **2012**, *81* (12), 124301. <https://doi.org/10.1143/JPSJ.81.124301>.
- (2) Zhou, Z.; Zhou, X.; Liu, Q.; Zhang, X.; Liu, H. Fixation of Zinc(II) Ion to Dioxygen in a Highly Deformed Porphyrin: Implications for the Oxygen Carrier Mechanism of Distorted Heme. *Org. Lett.* **2015**, *17* (16), 4078–4081. <https://doi.org/10.1021/acs.orglett.5b02010>.
- (3) Zhang, J.; Tang, M.; Chen, D.; Lin, B.; Zhou, Z.; Liu, Q. Horizontal and Vertical Push Effects in Saddled Zinc Porphyrin Complexes: Implications for Heme Distortion. *Inorg. Chem.* **2019**, *58* (4), 2627–2636. <https://doi.org/10.1021/acs.inorgchem.8b03219>.
- (4) Frisch, M. J.; Trucks, G. W.; Schlegel, H. B.; Scuseria, G. E.; Robb, M. A.; Cheeseman, J. R.; Scalmani, G.; Barone, V.; Petersson, G. A.; Nakatsuji, H. Gaussian 16, {Gaussian}. Inc., Wallingford CT **2016**, 2016.
- (5) Hehre, W. J.; Ditchfield, R.; Pople, J. A. Self—Consistent Molecular Orbital Methods. XII. Further Extensions of Gaussian—Type Basis Sets for Use in Molecular Orbital Studies of Organic Molecules. *J. Chem. Phys.* **1972**, *56* (5), 2257–2261. <https://doi.org/10.1063/1.1677527>.
- (6) Francl, M. M.; Pietro, W. J.; Hehre, W. J.; Binkley, J. S.; Gordon, M. S.; DeFrees, D. J.; Pople, J. A. Self-Consistent Molecular Orbital Methods. XXIII. A Polarization-Type Basis Set for Second-Row Elements. *J. Chem. Phys.* **1982**, *77* (7), 3654–3665. <https://doi.org/10.1063/1.444267>.
- (7) Hay, P. J.; Wadt, W. R. Ab Initio Effective Core Potentials for Molecular Calculations. Potentials for the Transition Metal Atoms Sc to Hg. *J. Chem. Phys.* **1985**, *82* (1), 270–283. <https://doi.org/10.1063/1.448799>.
- (8) Hay, P. J.; Wadt, W. R. Ab Initio Effective Core Potentials for Molecular Calculations. Potentials for K to Au Including the Outermost Core Orbitals. *J. Chem. Phys.* **1985**, *82* (1), 299–310. <https://doi.org/10.1063/1.448975>.